Enhancing Thermal and Mechanical Performance of Engineered Wood Product Adhesives using Novel Fire Retardant Nanoclays

by
Dr. Hale Oguzlu-Baldelli
Jason Yu
George Lee
Prof. Frank Lam
Prof. Feng Jiang

Sustainable Functional Biomaterials Laboratory
Department of Wood Science
Faculty of Forestry
University of British Columbia, Vancouver, B.C., Canada

Reporting Date
April 10th, 2021

Prepared for
Forestry Innovation Investment Ltd.
#1200-1130 Pender Street West
Vancouver, BC V6E 4A4, Canada

EXECUTIVE SUMMARY

One component PUR adhesive is widely used in engineered wood products applications, such as cross-laminated timber (CLT). However, the dramatic deterioration of PUR adhesive bond strength at elevated temperature can out tremendously threat for tall wood building, especially under fire. In this project, we are aiming to improving the bond strength of the PUR adhesive at high temperature by incorporating chemically modified halloysite to improve the poor interface between inorganic fillers and the polymer matrices. To improve the interaction with PUR (Loctite UR20 by Henkel®), the halloysite was chemically grafted with polymeric diphenylmethane diisocyanate (pMDI) (pMDI-H). The effect of adding pMDI modified halloysite to the PUR adhesives was investigated in terms of nanofiller dispersibility, thermal and mechanical properties of the pMDI-halloysite-PUR composite film, and the bonding shear strength of the glued Douglas fir and Spruce-Pine-Fir (SPF) shear blocks under different temperature.

Significant improvement of the bond shear strength can be observed with the addition of 5 and 10% of pMDI-modified PUR adhesive, and the key research findings are summarized as below,

a. pMDI can be successfully grafted onto hydroxylated halloysites to improve its dispersibility in one-component PUR adhesive;
b. Addition of pMDI-H into PUR adhesive can lead to improved glass transition temperature and storage modulus. In contrast, no significant enhancement was observed in h-H added PUR films due to the poor dispersibility;
c. Addition of up to 10% h-H and pMDI-H did not show significant change of the shear strength at 20 °C for both Douglas Fir and SPF;
d. Significant enhancement of shear strength at elevated temperature (60-100 °C) can be observed for 5% and 10% pMDI-H modified PUR adhesive, showing 17% improvement for Douglas Fir and 27-37% for SPF.

TABLE OF CONTENTS

List of Schemes

List of Figures

List of Tables

1. INTRODUCTION

With the increased development and application of engineering wood products (EWP), polyurethane adhesives have been widely used in different types of wood products, including oriented strand board (OSB), laminated strand lumber (LSL), and cross-laminated timber (CLT). There are several advantages for using polyurethane adhesives in these EWP including no formaldehyde emission and easy application and curing. Polyurethane adhesives are segmented copolymers composed of soft segment such as polyether or polyester polyol, and hard segments contain diisocyanate. The soft segment provides elasticity, whereas the hard segment contributes to strength and rigidity through physical crosslinking points.[1] Both one and two-components polyurethane adhesives are promoted as waterproof, formaldehyde-free, transparent systems, suitable for exterior and interior applications. One-component polyurethane adhesive (polyurethane reactive adhesive, PUR) is especially suitable for wood surface gluing because moisture in the wood can activate reaction with the isocyanate groups to complete the cure.[2]

Among various EWPs, cross-laminated timber (CLT) has been rising as a promising building material to replace high-rise concrete construction due to its environmental, structural, and constructional advantages leading to rapid onsite construction and the potential in the construction of tall buildings.[3] However, fire hazards, including ignition, delamination of the glue CLT, are the major challenges to commercialize engineered woods in the construction industry. Likewise, although PUR can provide excellent bond strength for CLT at room temperature, it suffers from weakened strength due to the softening of the glue layer at elevated temperature. During the initial stage of fire, the increased temperature could cause softening of the polyurethane adhesive, leading to severe glue failure that can may lead to structural collapse. Upon burning, the wood can char first, and then delamination can happen where fire-burnt lamella and parts detach from the main body of the timber, leading to structural collapse and continuous burning of the freshly exposed surface.[4] As a matter of fact, fire concern is the primary reason for limiting storey for tall wood building.[5] Therefore, there exist great opportunities in developing PUR adhesive that can withstand high temperature to meet the fire-resistant ratings for high-rise buildings.

Due to the high thermal stabilities, nanoclays, such as halloysites and montmorillonite, have been widely used as fire-retardant materials in varied materials including wood based products.[6-9] In addition to the flame retardancy, these inorganic nanomaterials have also been added into adhesives used in dentistry to improve the bond strength.[10, 11] It is also discovered that epoxy composite can be toughened by adding halloysites.[12] The thermal and mechanical performance of rigid polyurethane foam was also found to be enhanced with the addition of nanoclays and microcrystalline cellulose.[13] However, application of nanoclays in the wood adhesives have not been extensively investigated, and it is expected that the nanoclay can help to boost both the thermal and mechanical properties of wood adhesives. One challenge for incorporating nanoclays in wood adhesives is the uniform dispersibility, as severe aggregation can lead to internal defects that could reduce the bond strength.

In this project, we aimed to investigated how halloysite nanoclay can improve the bond strength of one-component PUR adhesive at elevated temperature. In order to improve the dispersibility of halloysite in the PUR adhesive, the halloysite was hydroxylated and then grafted with poly[(phenyl isocyanate)-co-formaldehyde] (pMDI) through surface activation and grating reaction. Grafting efficiency was investigated using Fourier-transform infrared spectroscopy (FTIR). The dispersibility of the halloysite in the PUR adhesive was further characterization using optical microscope, UV-Vis spectroscopy, rheometer, and transmission electron microscope (TEM). Thermal and thermomechanical performance of the halloysite modified PUR adhesives were investigated using Thermogravimetric Analysis (TGA) and Dynamic Mechanical Analysis (DMA). Lastly, the shear bond strength of Douglas Fir (DF) and Sprue-Pine-Fir (SPF) the halloysite modified PUR adhesives was investigated under four different temperature (20, 60, 80, and 100 ºC). Results showed significant improvement in the shear bond strength for pMDI modified PUR adhesive at 5 and 10% loading content as compared to the unmodified PUR adhesive.

2. MATERIALS AND METHODS

2.1 Materials

Halloysite (HNT) was kindly provided by Applied Minerals Inc. Poly[(phenyl isocyanate)-co-formaldehyde] (pMDI) (average Mn ~340), *N, N*-Dimethylformamide (DMF), hydrogen peroxide (H_2O_2) were purchased from Sigma Aldrich. Sodium hydroxide (NaOH) was purchased from Fischer Chemicals. Douglas fir and Spruce-Pine-Fir (SPF) dimension lumbers were provided by the Timber Engineering and Applied Mechanics (TEAM) Laboratory at UBC. The Loctite UR20 one-component PUR adhesive was initially kindly provided by Henkel®, and then purchased from ServCorp, Inc. (Grand Rapids, Michigan).

2.2 Synthesis of hydroxylated halloysite nanofillers (h-Hs)

Initially, HNTs were treated with hydrogen peroxide (H_2O_2) to remove organic impurities. Typically, 30.0 g of the as-received HNT was added into 200 ml 30% H_2O_2 aqueous solution and magnetically stirred for 1 h. The HNTs dispersion was then ultrasonicated for 10 min prior to centrifugation to separate HNTs from the liquid phase. The resultant purified HNTs (p-Hs) were dried at 110 °C for 12 h in an oven and then dried at room temperature in a vacuum oven for two days.[14] To increase the hydroxyl groups on the surface of HNTs, the p-Hs were then treated by NaOH. Typically, 20.00 g of p-Hs was dispersed in 1 L deionized water. Subsequently, 0.58 g NaOH was added, and the mixture was magnetically stirred for two days at room temperature. The resultant hydroxylated halloysite (h-H) solid phase was then separated by centrifugation and dialyzed in water for two weeks until the pH reached 7. The h-H suspensions were freeze-dried to prevent aggregation caused by hydrogen bonding between h-Hs.

2.3 Synthesis and characterization of pMDI-modified halloysite

Polymeric diphenylmethane diisocyanate (pMDI, Mn:340 Da) was used to modify halloysite to improve the compatibility of halloysite with PUR matrix for better dispersion. The reaction was carried out under a nitrogen (N_2) atmosphere to prevent the reaction of pMDI with moisture in the air. In a typical reaction, 2.0 g of pMDI was added to a DMF/h-Hs (90/10, w/w) suspensions and reacted for 24 h at 80 °C with continuous stirring. The product was isolated by centrifugation and washing with acetone and then dried under a vacuum environment at room temperature. The reaction between the isocyanate group and hydroxyl group is shown in **Scheme 1**.

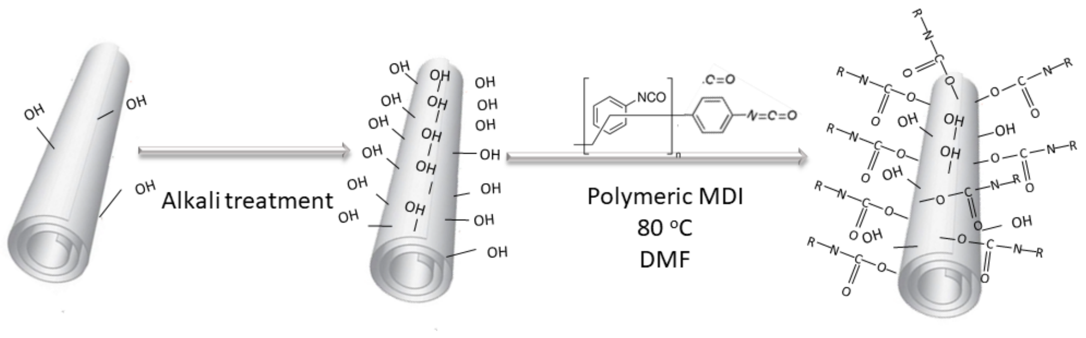

Scheme 1. Illustration of surface modification of halloysite including hydroxylation and pMDI grafting.

2.4 Characterization of h-H and pMDI-H

Very dilute (0.01 wt%) h-H (in water) and pMDI-H (in acetone) suspensions were deposited onto glow-discharged carbon-coated TEM grids (300-mesh copper, Formvar-carbon, Ted Pella Inc., Redding, CA). The excess liquid was removed by blotting with a filter paper to leave a thin suspension layer and dried under ambient condition. The samples were observed using a Hitachi H7600 transmission electron microscope (TEM) operated at an 80 kV accelerating voltage.

Unmodified halloysite, h-H, and pMDI-H were characterized by Fourier Transform Infrared Spectroscopy (INVENIO® S, Bruker Optics Pty. Ltd, Billerica, MA, USA). The spectra were recorded using the KBr pellet (halloysite:KBr ratio of 1:100) technique over 4000–400 cm^{-1} with an accumulation of 64 scans at 4 cm^{-1} resolution.

2.5 Viscosity of the halloysite modified PUR adhesives

PUR adhesive was modified by mixing h-H and pMDI-H with various concentrations (1, 5, and 10 wt%) at 80 ºC using high shear overhead stirrer at 1000 rpm for 1.5 hours under nitrogen atmosphere. The viscosity of pure and modified PUR adhesives was measured using a stress-controlled rheometer (AR-2000, TA Instruments, UK) on its continuous ramp mode, with parallel plate geometry (plate diameter = 25 mm, gap 1000 μm) at 25 °C

2.6 Casting of PUR Films

Both unmodified and modified PUR adhesives were used for film casting to investigate its dispersibility in the PUR matrix. Thin composite films were casted manually using a film applicator with 100 μm gap on a glass plate. The casted films were kept under ambient conditions for 24 hours to cure, and then peeled off the glass plate for further analysis. The thickness of the casted film was measured using a micrometer with resolution of 0.001 mm, and averaged from at least five measurement. All casted films were listed in Table 1.

Table 1. List of casted PUR and PUR/halloysite composite films

Sample Name	Filler Type	Filler content (wt%)	Thickness (μm)
PUR	n/a	-	45±2.0
1% h-H	h-HNTs	1	72±4.9
5% h-H	h-HNTs	5	81±2.1
10% h-H	h-HNTs	10	114±16.6
1% pMDI-H	pMDI-HNTs	1	35±0.8
5% pMDI-H	pMDI-HNTs	5	50±0.0
10% pMDI-H	pMDI-HNTs	10	62±0.3

2.7 Dispersibility of various inorganic fillers in PUR matrix

Dispersibility of h-H and pMDI-H nanofillers in the PUR matrix was investigated using optical microscopy and UV-Vis Spectroscopy. PUR films were observed in the reflective light field mode with a Nikon Eclipse LV100POL optical microscope equipped with a camera and NIS microscope imaging software. Cary 60 UV–vis spectrophotometer (Agilent Technologies, Santa Clara, CA, USA) was used to measure the transmittance of the PUR films at wavelengths of 200–500 nm.

2.8 Thermal and thermomechanical properties of PUR films

Thermal properties of the PUR films were analyzed with a thermogravimetric analyzer (TGA; TA Instruments Q500, New Castle, USA). Samples were vacuum dried overnight before analysis. PUR films were heated from 30 °C to 500 °C at a rate of 10 °C/min under a constant flow of nitrogen (60 ml/min).

Glass transition temperatures, loss modulus, and storage modulus values of PUR films were determined using a dynamic mechanical analyzer (Q800, TA Instruments). Dynamic mechanical analysis (DMA) was performed in tension mode at a frequency of 1 Hz from -90 °C to 200 °C at a heating rate of 3 °C/min.

2.9 Mechanical properties of shear block

The bond shear strength was measuring using a shear block manufactured from both Douglas Fir (DF) and Spruce-Pine-Fir (SPF) as shown in **Scheme 2** according to ASTM D905-08 and ASTM D7247-17.

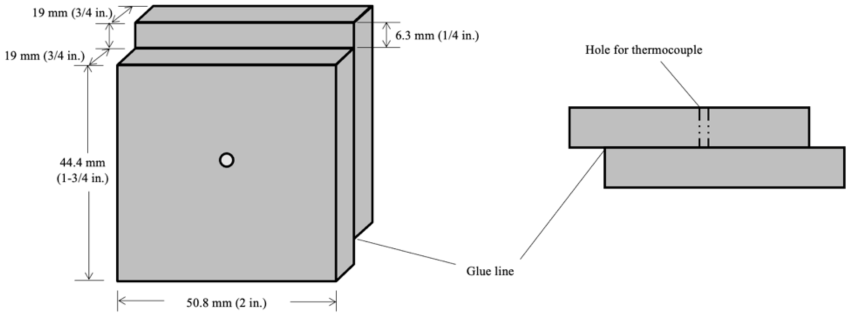

Scheme 2. Schematic illustration of a shear block used for shear bond strength testing.

The DF and SPF lumbers were firstly cut into blocks of 63.5 x 19 x 550 mm^3 and planed before applying adhesive. Both unmodified and modified PUR adhesives were applied to newly planed blocks at approximately 150 g/m^2 adhesive loading amount. The glued lumbers were then clamped for over 18 hours to ensure complete cure of the adhesives, and then cut into shear block as in Scheme 2. A small hole is drilled in the center for each sample to install thermocouple and monitor the glue line temperature during mechanical testing. Afterward, the specimens were put into the conditioning room (20°C and 65% relative humidity) for over 24 hours before testing.

Mechanical shear testing was carried out under 20, 60, 80, and 100 °C using MTS Flextest GT Structural Test Machine (**Figure 1**). For testing at elevated temperature, the specimens were preheated in an oven for around 90 min until the glue line temperature reaches the target temperature. During testing, a continuously increasing shear force was applied with a loading rate of 5 mm (0.2 in) /min until the failure of the blocks. Peak load and shear strength can be obtained from the stress-strain curves. The broken specimens were taken to determine the wood failure percentage of the bonding area after testing. For each adhesive-temperature combination, 30 shear block specimens were tested.

The one-way analysis of variance (ANOVA) was performed with IBM® SPSS® (statistical package for the social science) data analysis software. The assumption of homogeneity of variance was tested right before the analysis. If the assumption holds, then classic ANOVA would be carried out to determine the significance of difference among groups, while the Bonferroni test will show the comparison between every two groups. If the assumption is not valid, Welch's t-test and Brown–Forsythe test will replace the classic ANOVA and give the results together with the Tamhane comparison test. After the testing, those groups with p-values lower than 0.05 (95% confidence interval) would be considered to have significant differences compared with the control group.

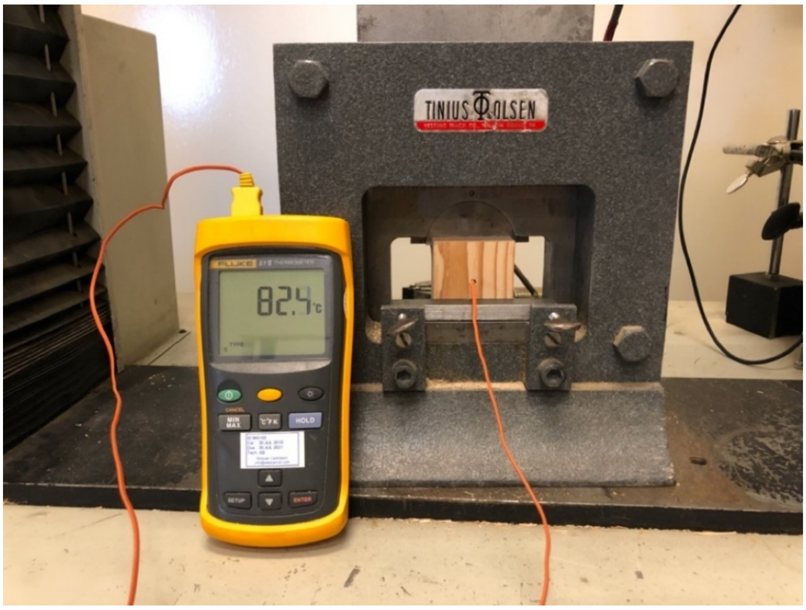

Figure 1. Photo of shear testing of the shear block with a thermocouple measuring the glue line temperature.

3. RESULTS AND DISCUSSION

3.1 Characterization of modified Halloysite

3.1.1 FTIR spectra of h-H and pMDI-H

The surface of halloysite was initially hydroxylated to increase the surface hydroxyl content, which can be further used for grating of pMDI through urethane linkage formed between the isocyanate group of pMDI and the hydroxyl of h-Hs (Scheme 1). Sodium hydroxide treatment of pristine halloysite results in the formation of hydroxyl groups on the surface of halloysite, and the addition of surface hydroxyl groups can be clearly observed from the FTIR spectra of pristine halloysite (p-H) and hydroxylated halloysite (h-H) (**Figure 2a**). For halloysite, the characteristic peaks at 3690 $cm^{-1}$and 3619 cm^{-1} can be ascribed to Al_2OH stretching, indicating the hydroxyl groups inside the tubes. A broad peak in the 3500–3200 cm^{-1} range with a shoulder peak at 3424 cm^{-1} is ascribed to Si-OH vibration, indicating the hydroxyl group attached on the surface of silicate layers. After hydroxylation reaction, the shoulder peak at 3424 cm^{-1} becomes more prominent, indicating more surface hydroxyls on the Si-OH are introduced by NaOH activation.

Successful grafting of pMDI onto the surface of h-H can be further corroborated from the FTIR spectra as shown in Figure 2b. After modification, the shoulder peak in the 3500–3200 cm^{-1} range becomes reduced due to the reaction between the isocyanate group and the hydroxyl group. In addition, absorbency peaks at around 1654 cm^{-1}, 1508 cm^{-1}, and 1418 cm^{-1} appeared in the pMDI-H, which can be ascribed to the phenyl stretching in the grafted pMDI. Therefore, FTIR results confirmed that pMDI is successfully grafted onto the hydroxylated halloysite.

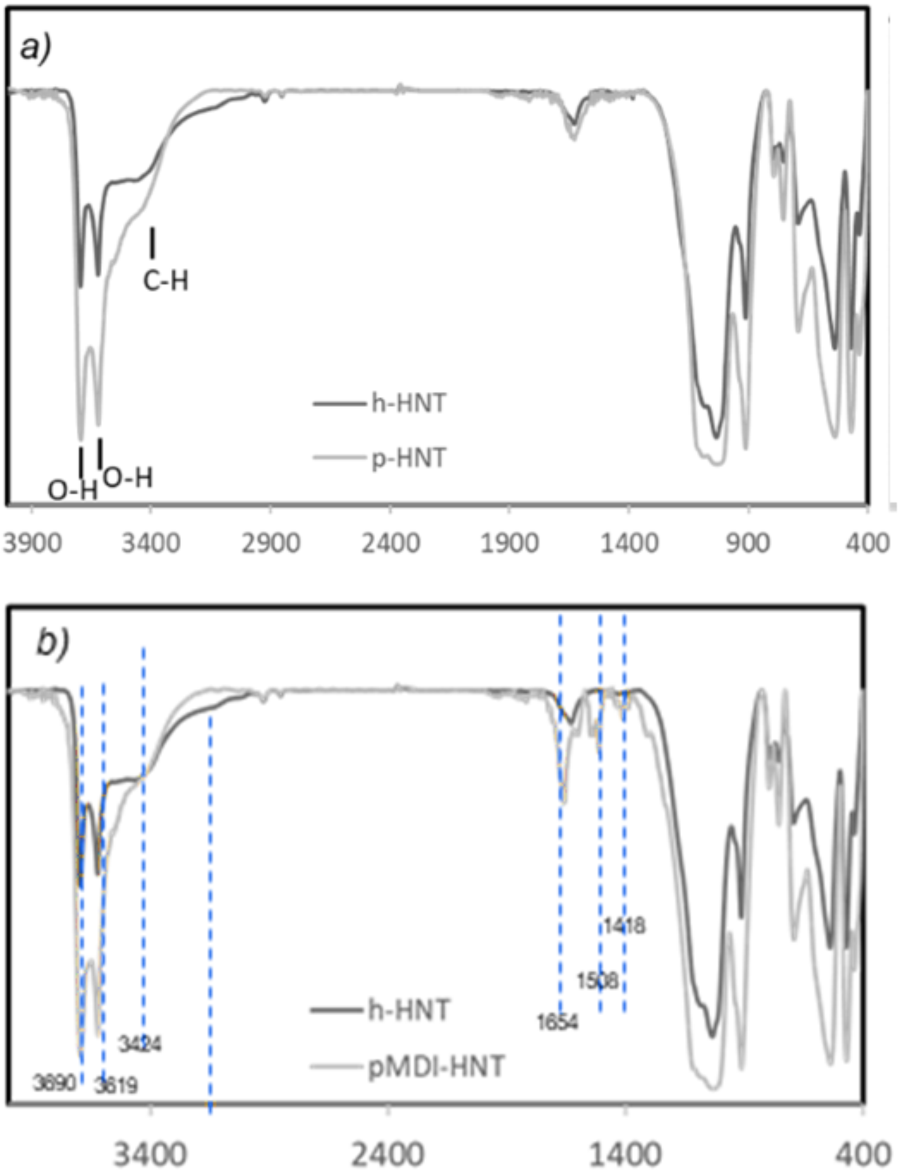

Figure 2. FTIR Spectra of (b) p-Hs and h-Hs.

3.1.2 Morphologies of h-H and pMDI-H

Both h-H and pMDI-H were visualized under TEM for examine the morphological change before and after pMDI modification (**Figure 3**). The diameter of h-H is around 20-30 nm, and the length is around 100-200 nm (Figure 3a). Furthermore, the hallow tube structure of h-Hs was preserved after hydroxylation reaction, indicating that NaOH treatment did not change the morphology of halloysites. Compared to h-Hs, pMDI-Hs showed similarly tubular structure (Figure 3b). However, more severe aggregation can be observed for pMDI-H, which might be due to the reaction of surface pMDI groups with moisture during sample preparation, leading to crosslinking between adjacent pMDI-Hs.

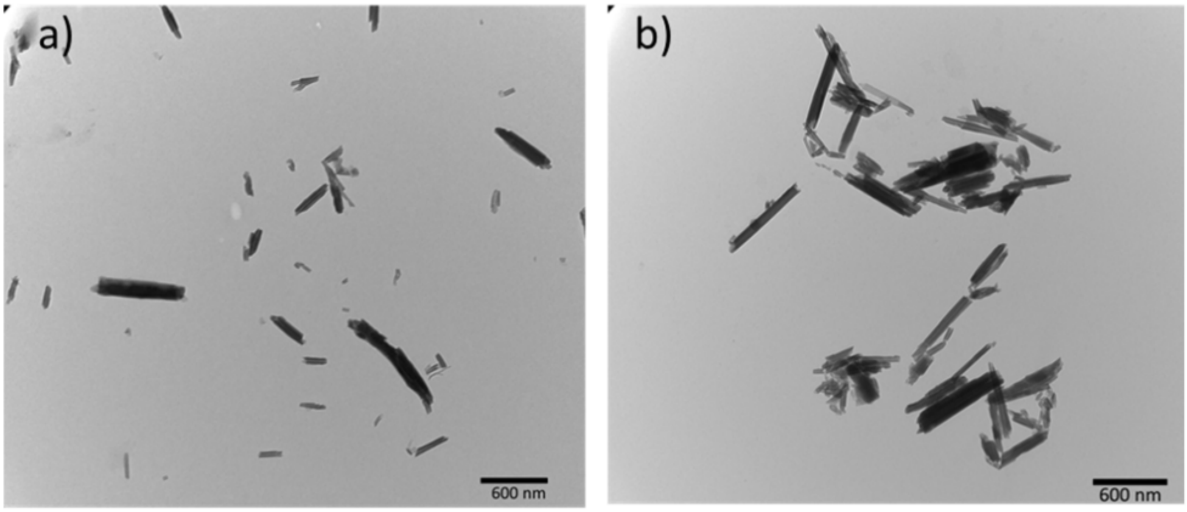

Figure 3. TEM images of (a) h-H and (b) pMDI-H.

3.2 Dispersibility of h-H and pMDI-H in PUR adhesive

3.2.1 Rheological properties of PUR adhesives

Rheological properties, especially viscosity, can be used to indicate the dispersibility of nanofillers in polymer matrix. The viscosity of all PUR adhesives was measured at increased shear rate and shown in **Figure 4**. All PUR adhesives presented Newtonian behavior. Addition of halloysite into PUR significantly increased the viscosity and such increase is positively correlated to the amount of halloysite in the adhesive. Under low concentration of 1%, both h-H and pMDI-H modified PUR adhesive showed similar viscosity values that are slightly higher than the pure PUR adhesive. At 5% halloysite, the viscosity of pMDI-H modified PUR adhesive is higher than that of h-H modified PUR. Further increasing the halloysite content to 10% led to dramatic increase in the viscosity of h-H modified PUR adhesive. The much higher viscosity of 10% h-H modified PUR adhesive suggested more severe aggregation of the halloysite.

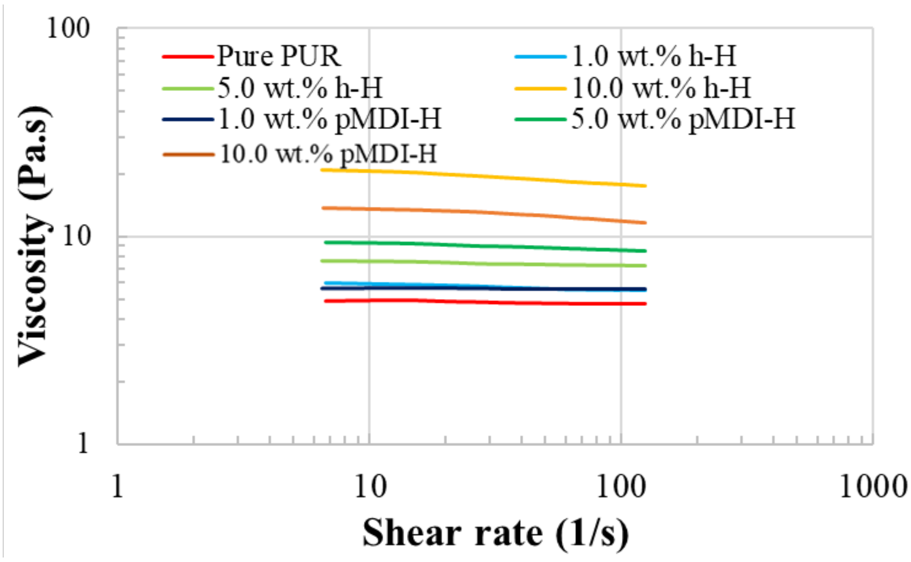

Figure 4. Viscosity of modified PUR adhesives.

3.2.2 Optical Microscope images of PUR films

To further investigate the dispersibility of h-H and pMDI-H in the PUR adhesives, thin film was casted onto glass using a manual film applicator with gap of 100 μm. It can be observed that the film thickness increased with increasing halloysite filler (Table 1), which can be ascribed to the higher viscosity of the halloysite modified PUR. Pure PUR casted film showed high transparency to reveal the UBC logo underneath, indicating homogeneous film morphology (Figure 5). Similar appearance can be observed for PUR film containing 1% h-H and pMDI-H, as the low nanofiller content did not significantly affect the film morphology. However, the composite PUR film containing 5% and 10% h-H appeared as yellowish color with diminished transparency, suggesting reduced transparency caused by the nanofiller aggregation (Figure 5a). On the other hand, although the composite PUR film containing 5% and 10% pMDI-H also revealed reduced transparency, it is not as severe as the h-H modified ones.

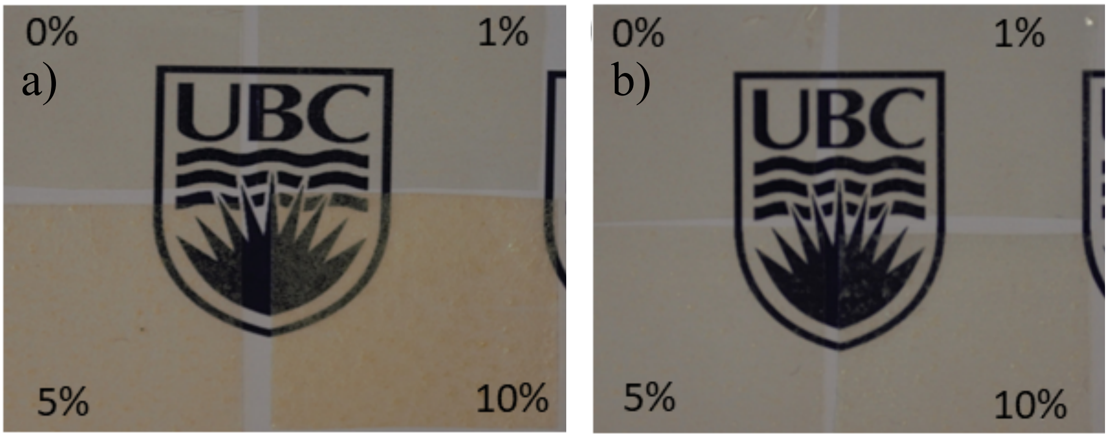

Figure 5. Photos of casted PUR film with (a) h-Hs and (b) pMDI-Hs.

Optical microscope images are further used to visualize the dispersibility of halloysites in the PUR matrix (**Figure 6**). Compared to pure PUR film, which shows uniform morphology, all halloysite modified PUR films demonstrate aggregates under optical microscope. Big aggregate of approximately 50 μm wide can be observed in all h-H modified PUR film, indicating poor dispersibility of the halloysite in the PUR matrix, which is consistent with the previous optical images. As compared to the h-H modified PUR film, pMDI-H modified PUR films showed much less aggregate under the optical microscope, revealing better dispersibility after pMDI modification. However, such large aggregates can still be observed at high halloysite content as achieving nano-scaled dispersion of the nanofillers has always been a challenge.

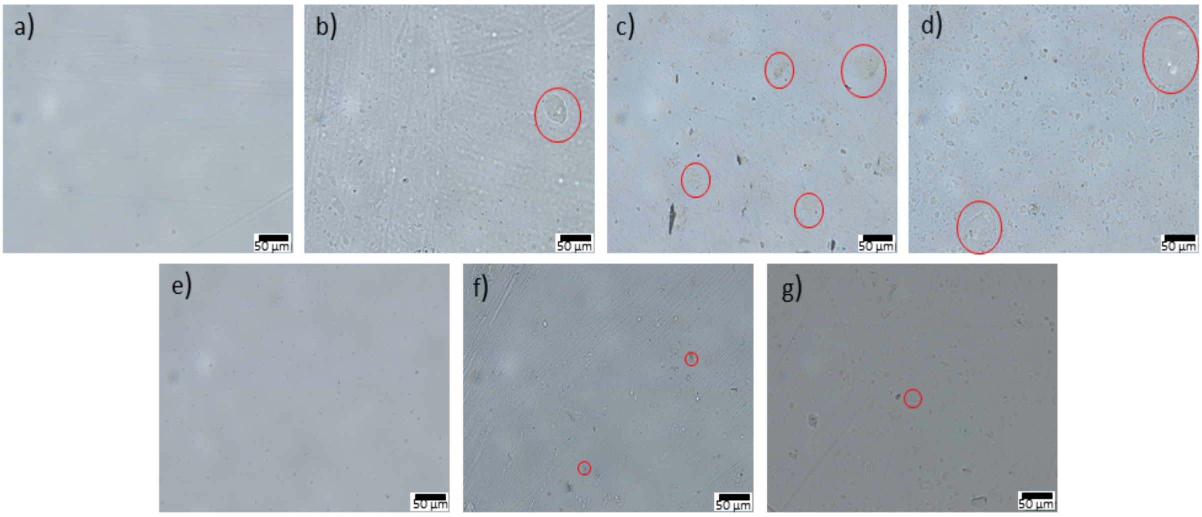

Figure 6. Optical microscope images of PUR films (a) without any additive, including (b)1%, (c) 5%, (d) 10% h-Hs, and (e)1%, (f) 5%, (g) 10% pMDI-H.

3.2.3 UV-Vis transmittance of PUR films

Optical transmittance of the PUR. Films were measured to quantify the transmittance values (**Figure 7**). Unmodified PUR film showed highest transmittance value at 500 nm, followed by the two PUR/halloysite composite films with 1% h-H and 1% pMDI-H. The 5% pMDI-H and 10% pMDI-H modified PUR film showed similar transmittance value, and the 10% h-H showed lowest transmittance value, indicating the poor dispersibility of the hydroxylated halloysite. Therefore, the optical transmittance value is consistent with the visual appearance and the optical microscope images, indicating that pMDI modification can improve the dispersity of halloysite in the PUR film.

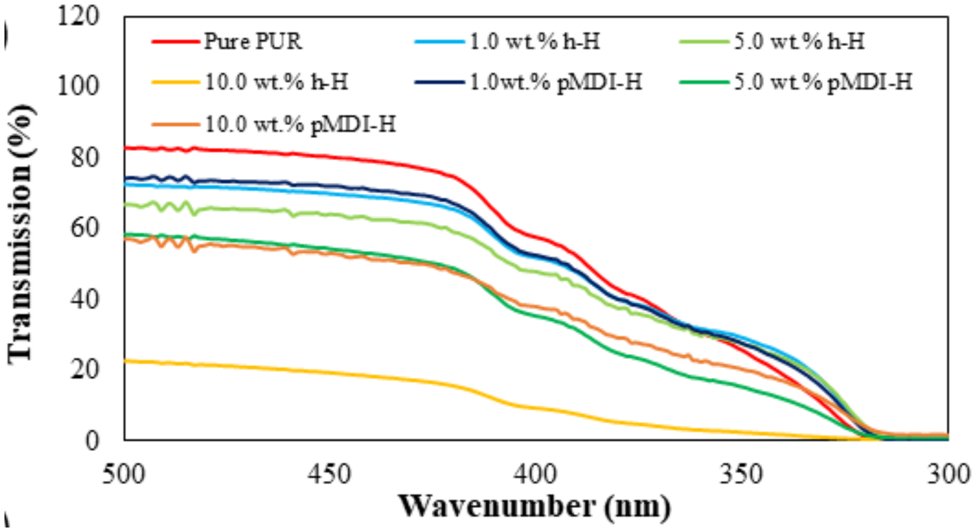

Figure 7. UV-vis spectra of PUR films.

3.3 Thermal and dynamic mechanical properties of PUR films

TGA and derivative thermogravimetric (DTG) curves versus temperature graph are shown in **Figure 8** and the thermal properties are summarized in **Table 2**. With increase halloysite contents, less weight loss can be observed as the halloysite cannot be thermally decomposed at the investigated temperature. In the timber structure, higher char residue can benefit the fire retardance performance, which can be regarded as one advantage of halloysite modification. In addition, the 1st derivative peak faded with the addition of 5.0 and 10 wt.% pMDI-H and 10.0 wt.% h-H, indicating an enhancement in thermal stability of PUR adhesive systems.

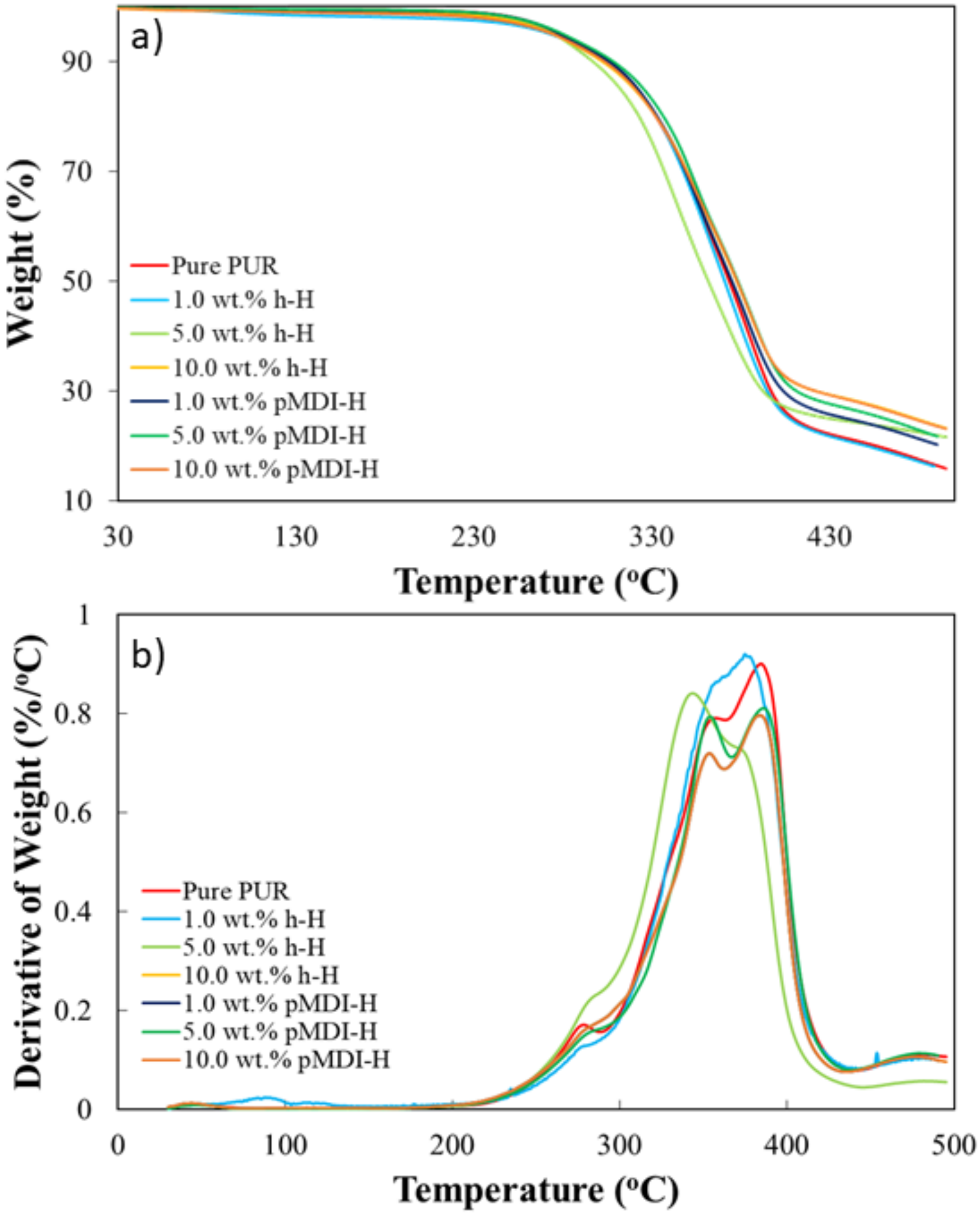

Figure 8. Thermogravimetric analysis (TGA) and derivative thermogravimetric (DTG) curves of (a) h-halloysite modified one component PUR adhesive.

Table 2. Thermal properties of PUR adhesive with the addition of h-H and pMDI-Hs at various loading content.

Sample Name	**Weight loss (%)**	**1^{st} T_{max} (°C)**	**2^{nd} T_{max} (°C)**	**3^{rd} T_{max} (°C)**	**Tg_{α} (°C)**	**Tg_{β} (°C)**
Pure PUR	83.95	277.10	349.48	384.61	-38.61	62.86
1% h-H	84.15	275.43	356.76	375.76	51.40	65.09
5% h-H	78.05	N/A	343.57	373.78	-7.82	59.54
10% h-H	76.03	278.95	353.72	384.2	-13.29	69.09
1% pMDI-H	79.88	279.21	354.69	383.46	-22.76	55.08
5% pMDI-H	78.47	N/A	353.08	385.44	-10.70	70.15
10% pMDI-H	76.54	N/A	352.16	384.39	-12.17	72.36

The DMA results are shown in **Figure 9**, including storage modulus, loss modulus, and tan δ. Glass transition temperatures (Tg) were calculated by determining the maximum peak height of loss modulus curves (Table 2). Similar to TGA, h-H addition did not show any trend in Tg values due to the heterogenicity of the internal structure. However, a drastic increase in Tg values of pMDI-H added PUR films was observed due to the good level of dispersion of fillers. Especially, the addition of 5 and 10% pMDI-H elevated the values of Tgα and Tgβ around 26 °C and 10 °C, respectively. The significant enhancement was also seen in 10% h-H added films which are only related to filler amount because there is no improvement in moduli values of that sample In other words, both thermal and mechanical improvement can be observed when fillers are well dispersed in the matrix.

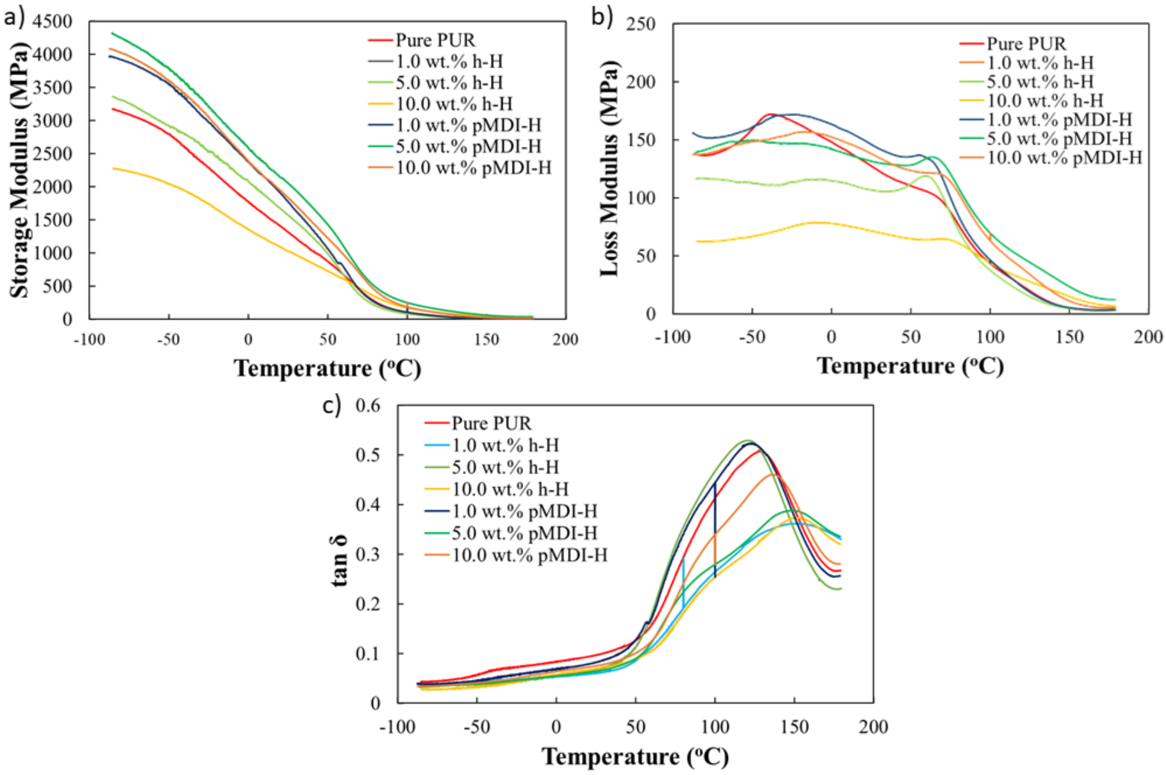

Figure 9. Dynamic mechanical analysis curves of PUR films with various halloysite contents: (a) storage modulus, (b) loss modulus, and (c) and tan δ.

Figure 10 shows the storage and loss modulus values at a certain temperature. The storage and loss modulus value of 10% h-H modified PUR films with pure PUR films at 20 °C, 60 °C,80 °C, and 100 °C were all much lower than pure PUR films. This coukld be due to the severe aggregation of h-H in the matrix. In addition, there is no trend in the change of loss moduli values in h-H modified PUR films while there is an improvement in storage modulus values up to 5% of h-H addition. In the case of pMDI-H modified PUR film, storage and loss moduli values were all increased as compared to the pure PUR film, indicating an enhancement in thermomechanical properties of pMDI-H modified PUR films.

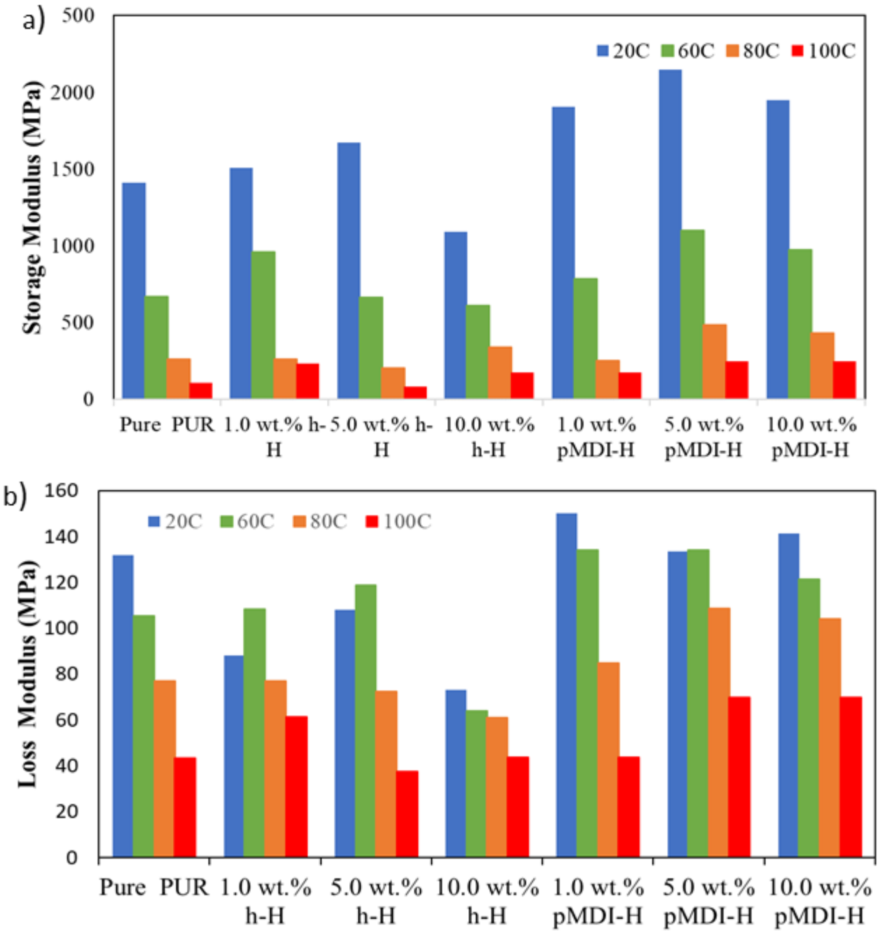

Figure 10. (a) Storage moduli and (b) loss moduli at varied temperatures (20 ºC , 60 ºC, 80 ºC and 100 ºC) of PUR films with various filler content.

3.4 Mechanical properties of the glued shear block

3.4.1 Douglas fir

Douglas fir was selected as the species for testing the bond shear strength of the unmodified and modified PUR adhesives, and the data, including shear strength, percentage of wood failure are presented in **Table 3-6**. The shear strength values at different temperature are plotted in **Figure 11- 14**. A one-way ANOVA (analysis of variance) at a significance level of 5% was performed to compare the differences between the control group and halloysite modified PUR adhesive groups to determine the significance of the difference (**Table 7**).

For the specimens tested under 20 °C, the *p*-value of the ANOVA result for shear strength of all halloysite modified PUR adhesives and unmodified PUR adhesive are 1. It can be concluded that there is no significant difference among the unmodified and modified adhesive samples under room temperature, indicating that adding h-halloysite and pMDI-halloysite powder did not deteriorate the adhesive performance. While for the samples under three different elevated temperatures (60 °C, 80 °C, and 100°C), a statistically significant difference for adding halloysite can be observed. The significance level (p-value) for different temperature groups of data was always lower than 0.01. When increasing to an elevated temperature, the shear strength and wood failure percentage for unmodified PUR adhesive both decreased significantly. When the temperature was reaching 60 °C, shear strength decreased from 10.77 MPa to 7.08 MPa, which means a 34% shear strength loss and even higher loss when getting 80°C, and 100°C. After Comparing with unmodified PUR adhesive in ANOVA, it can be noticed that only 5% pMDI-H and 10% pMDI-H have statistically significant difference with unmodified PUR. Compared with the unmodified PUR, their p-values are always lower than 0.01, while at 80 °C, the p-value was even lower than 0.001 for 5% pMDI-H.

1% h-halloysite and 5% h-halloysite had almost no difference compared with the unmodified PUR group under different temperatures. The ANOVA result can confirm that while reaching 80 °C and 100 °C, there’s no significant difference between the three groups of data (p-value around 0.5). For 1% pMDI-H and 10% h-H, a minor increase in thermal stability can be obtained from the shear strength and wood failure data, even though their ANOVA value showed no significant difference. Meanwhile, 5% pMDI-H and 10% pMDI-H modified adhesives always had the highest remaining shear strength and wood failure percentage among all groups under different elevated temperatures. Overal, pMDI-H modified PUR adhesive showed approximately 16% enhancement of the shear strength at 5% and 10% loading amount as compared to unmodified PUR adhesive.

It should be noted that the evaluation of the percentage of wood failure would not be entirely accurate since the splitting of the cracked samples sometimes created a new failure plane instead of the actual one. Thus, the percentage of wood failure can only be used as additional proof of better performance. For example, wood failure for 5%

pMDI-H and 10% pMDI-H modified adhesives at 100 °C were both over 70%, while for unmodified PUR was only 63.45%, which means modified adhesives had better bonding performance since more cracks appearing at wood phase (**Figure 15**).

Table 3. Statistics of the adhesive Bonding Tests-DF at 20 ºC.

Category	DF-PUR (20 °C)			DF-PUR+1%h-H (20 °C)			DF-PUR+5%h-H (20 °C)			DF-PUR+10%h-H (20 °C)			DF-PUR+1% pMDI-H (20 °C)			DF-PUR+5% pMDI-H (20 °C)			DF-PUR+10% pMDI-H (20 °C)		
	Peak Load (N)	Shear Strength (MPa)	Wood Failure (%)	Peak Load (N)	Shear Strength (MPa)	Wood Failure (%)	Peak Load (N)	Shear Strength (MPa)	Wood Failure (%)	Peak Load (N)	Shear Strength (MPa)	Wood Failure (%)	Peak Load (N)	Shear Strength (MPa)	Wood Failure (%)	Peak Load (N)	Shear Strength (MPa)	Wood Failure (%)	Peak Load (N)	Shear Strength (MPa)	Wood Failure (%)
Aver.	21554	10.77	93.71%	21870	10.98	95.13%	21571	10.74	93.02%	21249	10.47	93.94%	21091	10.48	94.58%	21121	10.70	95.04%	21533	10.68	95.80%
Stdev	2621	1.34	7.00%	2657	1.37	7.38%	3102	1.58	8.00%	2650	1.30	6.54%	2632	1.33	5.39%	2688	1.40	8.02%	2281	1.16	3.99%
Max	27651	14.21	100.00%	25543	13.01	100.00%	27584	13.71	100.00%	27275	13.46	100.00%	25597	12.79	100.00%	25771	13.26	100.00%	25610	12.60	100.00%
Min	15906	8.14	77.50%	15543	7.71	76.25%	15933	7.99	71.25%	16631	8.27	71.25%	16503	8.24	83.75%	14765	7.38	70.00%	16416	8.12	80.00%
Count	30	30	30	30	30	30	30	30	30	30	30	30	30	30	30	30	30	30	30	30	30

Table 4-1. Statistics of the adhesive Bonding Tests-DF at 60 ºC with unmodified PUR and h-halloysite (h-H) modified PUR.

Category	DF-PUR (60 °C)				DF-PUR+1%h-h (60 °C)				DF-PUR+5%h-h (60 °C)				DF-PUR+10%h-h (60 °C)			
	Bond Surface Temp (°C)	Peak Load (N)	Shear Strength (MPa)	Wood Failure (%)	Bond Surface Temp (°C)	Peak Load (N)	Shear Strength (MPa)	Wood Failure (%)	Bond Surface Temp (°C)	Peak Load (N)	Shear Strength (MPa)	Wood Failure (%)	Bond Surface Temp (°C)	Peak Load (N)	Shear Strength (MPa)	Wood Failure (%)
Aver.	59.21	14234	7.08	81.25%	61.07	15250	7.60	57.50%	60.20	14909	7.44	77.08%	61.01	15739	7.87	83.06%
Stdev	2.79	2211	1.11	16.13%	2.58	1948	0.96	14.72%	3.39	2803	1.42	16.27%	2.48	3135	1.57	14.52%
Max	64.90	18221	9.01	100.00%	64.90	18725	9.23	90.00%	66.20	19255	9.60	100.00%	64.90	21436	10.70	100.00%
Min	55.20	8314	4.13	47.50%	56.00	9302	4.58	35.00%	52.80	8894	4.46	48.75%	56.00	7804	3.93	50.00%
Count	30	30	30	30	30	30	30	30	30	30	30	30	30	30	30	30

Table 4-2. Statistics of the adhesive Bonding Tests-DF at 60 ºC with pMDI-halloysite (pMDI-H) modified PUR.

Category	DF-PUR+1% pMDI (60 °C)				DF-PUR+5% pMDI (60 °C)				DF-PUR+10% pMDI (60 °C)			
	Bond Surface Temp (°C)	Peak Load (N)	Shear Strength (MPa)	Wood Failure (%)	Bond Surface Temp (°C)	Peak Load (N)	Shear Strength (MPa)	Wood Failure (%)	Bond Surface Temp (°C)	Peak Load (N)	Shear Strength (MPa)	Wood Failure (%)
Aver.	59.74	15262	7.67	77.04%	61.53	16437	8.29	83.13%	60.33	16375	8.16	83.17%
Stdev	2.26	1482	0.73	18.91%	2.09	2522	1.30	19.32%	2.55	2406	1.18	19.17%
Max	64.50	17798	8.88	100.00%	64.90	21510	10.83	100.00%	64.80	20798	10.26	100.00%
Min	55.50	12832	6.38	31.25%	57.50	12335	6.20	17.50%	55.00	11832	5.92	37.50%
Count	30	30	30	30	30	30	30	30	30	30	30	30

Table 5-1. Statistics of the adhesive Bonding Tests-DF at 80 ºC with unmodified PUR and h-halloysite (h-H) modified PUR.

Category	DF-PUR (80 °C)				DF-PUR+1%h-h (80 °C)				DF-PUR+5%h-h (80 °C)				DF-PUR+10%h-h (80 °C)			
	Bond Surface Temp (°C)	Peak Load (N)	Shear Strength (MPa)	Wood Failure (%)	Bond Surface Temp (°C)	Peak Load (N)	Shear Strength (MPa)	Wood Failure (%)	Bond Surface Temp (°C)	Peak Load (N)	Shear Strength (MPa)	Wood Failure (%)	Bond Surface Temp (°C)	Peak Load (N)	Shear Strength (MPa)	Wood Failure (%)
Aver.	80.00	13590	6.77	68.94%	80.22	13412	6.72	64.50%	78.67	14152	7.07	77.07%	79.87	15033	7.53	82.07%
Stdev	3.04	2019	1.02	14.69%	3.36	2605	1.29	10.00%	2.90	2792	1.42	16.79%	2.99	1965	0.96	16.35%
Max	84.80	17027	8.38	100.00%	84.90	17436	8.79	85.00%	84.90	18382	9.33	100.00%	84.80	17718	8.77	97.50%
Min	75.30	8137	4.02	47.50%	75.30	9007	4.49	43.75%	75.00	8612	4.37	37.50%	75.30	9286	4.70	42.50%
Count	30	30	30	30	30	30	30	30	30	30	30	30	30	30	30	30

Table 5-2. Statistics of the adhesive Bonding Tests-DF at 80 ºC with pMDI-halloysite (pMDI-H) modified PUR.

	DF-PUR+1% pMDI (80 °C)				DF-PUR+5% pMDI (80 °C)				DF-PUR+10% pMDI (80 °C)			
Category	Bond Surface Temp (°C)	Peak Load (N)	Shear Strength (MPa)	Wood Failure (%)	Bond Surface Temp (°C)	Peak Load (N)	Shear Strength (MPa)	Wood Failure (%)	Bond Surface Temp (°C)	Peak Load (N)	Shear Strength (MPa)	Wood Failure (%)
Aver.	79.93	14373	7.20	75.75%	78.87	15615	7.91	77.96%	79.15	15584	7.84	84.13%
Stdev	2.85	1541	0.75	18.54%	2.18	1539	0.78	12.72%	2.54	1952	1.00	12.69%
Max	84.20	18154	9.02	100.00%	83.80	18349	9.30	100.00%	83.90	18631	9.26	100.00%
Min	75.00	11080	5.50	28.75%	75.60	12664	6.28	51.25%	75.30	11060	5.58	56.25%
Count	30	30	30	30	30	30	30	30	30	30	30	30

Table 6-1. Statistics of the adhesive Bonding Tests-DF at 100 ºC with unmodified PUR and h-halloysite (h-H) modified PUR.

	DF-PUR (100 °C)				DF-PUR+1%h-h (100 °C)				DF-PUR+5%h-h (100 °C)				DF-PUR+10%h-h (100 °C)			
Category	Bond Surface Temp (°C)	Peak Load (N)	Shear Strength (MPa)	Wood Failure (%)	Bond Surface Temp (°C)	Peak Load (N)	Shear Strength (MPa)	Wood Failure (%)	Bond Surface Temp (°C)	Peak Load (N)	Shear Strength (MPa)	Wood Failure (%)	Bond Surface Temp (°C)	Peak Load (N)	Shear Strength (MPa)	Wood Failure (%)
Aver.	100.36	13329	6.63	63.45%	98.63	13131	6.65	59.96%	99.72	13718	6.92	54.38%	99.60	14430	7.27	73.71%
Stdev	2.68	1835	0.88	20.24%	2.60	2542	1.28	18.62%	2.92	2244	1.13	27.05%	2.73	2056	1.06	19.82%
Max	104.50	16053	7.81	100.00%	104.40	17141	8.73	100.00%	104.80	18731	9.35	95.00%	104.90	17463	8.87	100.00%
Min	95.90	9101	4.62	32.50%	95.30	8730	4.40	25.00%	95.00	9058	4.60	10.00%	95.20	9176	4.57	37.50%
Count	30	30	30	30	30	30	30	30	30	30	30	30	30	30	30	30

Table 6-2. Statistics of the adhesive Bonding Tests-DF at 100 ºC with pMDI-halloysite (pMDI-H) modified PUR.

Category	DF-PUR+1% pMDI (100 °C)				DF-PUR+5% pMDI (100 °C)				DF-PUR+10% pMDI (100 °C)			
	Bond Surface Temp (°C)	Peak Load (N)	Shear Strength (MPa)	Wood Failure (%)	Bond Surface Temp (°C)	Peak Load (N)	Shear Strength (MPa)	Wood Failure (%)	Bond Surface Temp (°C)	Peak Load (N)	Shear Strength (MPa)	Wood Failure (%)
Aver.	99.79	14392	7.25	66.90%	99.26	15117	7.70	73.79%	99.74	15205	7.72	71.81%
Stdev	3.04	2181	1.10	23.01%	2.58	1748	0.88	12.88%	2.36	2131	1.07	19.72%
Max	104.70	18805	9.55	100.00%	104.80	19255	9.78	100.00%	104.60	19362	9.71	100.00%
Min	95.00	10087	5.02	21.25%	95.60	12054	6.16	47.50%	95.80	11067	5.72	30.00%
Count	30	30	30	30	30	30	30	30	30	30	30	30

Table 7. Comparison among groups with ANOVA for DF samples.

Control group	Samples	20 °C			60 °C			80 °C			100 °C		
		Mean difference	Stdev	p-Value	Mean difference	Stdev	p-Value	Mean difference	Stdev	p-Value	Mean difference	Stdev	p-Value
PUR	1% h-H	-0.2042	0.351	1	-0.52147	0.268	0.703	0.05723	0.3	1	-0.02026	0.275	1
	5% h-H	0.02733	0.349	1	-0.35924	0.33	0.999	-0.29504	0.322	1	-0.28654	0.275	1
	10% h-H	0.3023	0.358	1	-0.78653	0.35	0.462	-0.75743	0.257	0.093	-0.6443	0.275	0.425
	1% pMDI-H	0.28941	0.351	1	-0.5901	0.241	0.318	-0.42357	0.231	0.793	-0.62016	0.275	0.533
	5% pMDI-H	0.06925	0.351	1	-1.21440	0.312	0.006**	-1.13382	0.234	<0.001***	-1.06624	0.275	0.003**
	10% pMDI-H	0.09302	0.351	1	-1.08437	0.296	0.011*	-1.06717*	0.261	0.003**	-1.08715	0.275	0.002**

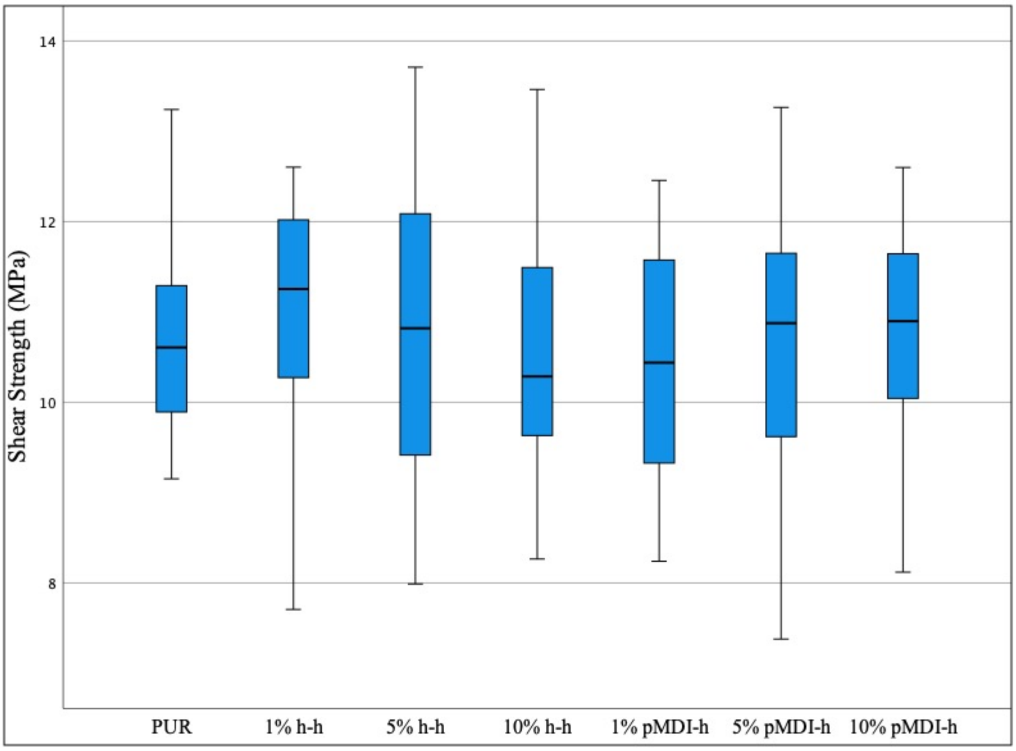

Figure 11. Shear Strength of unmodified and modified PUR at 20 °C

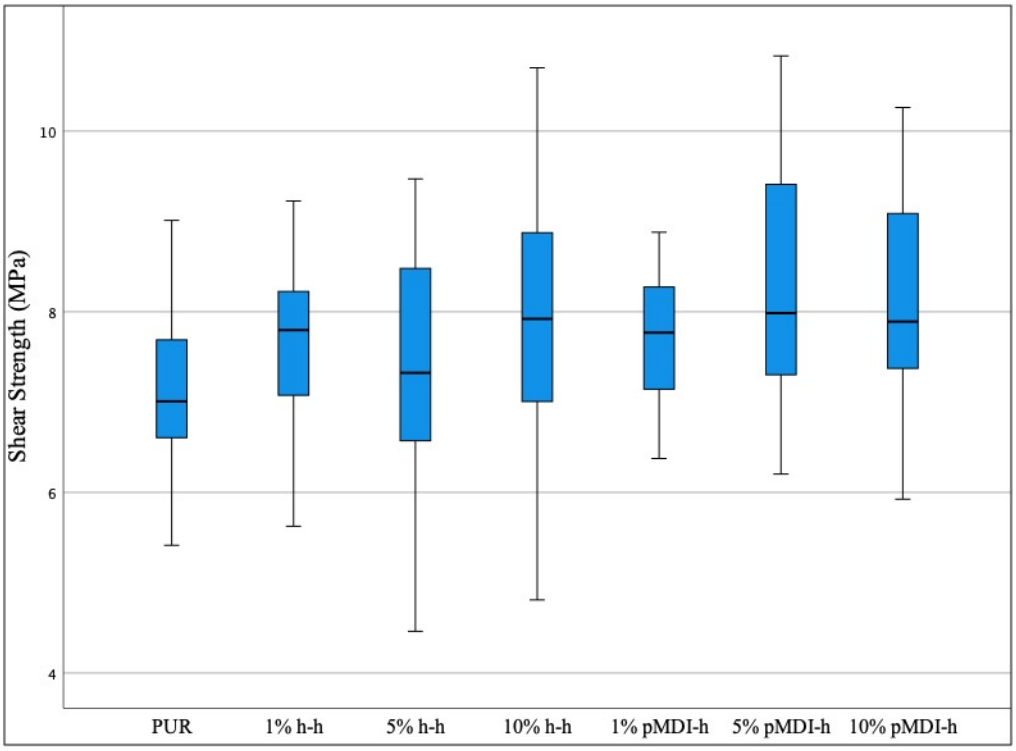

Figure 12. Shear Strength of unmodified and modified PUR at 60 °C

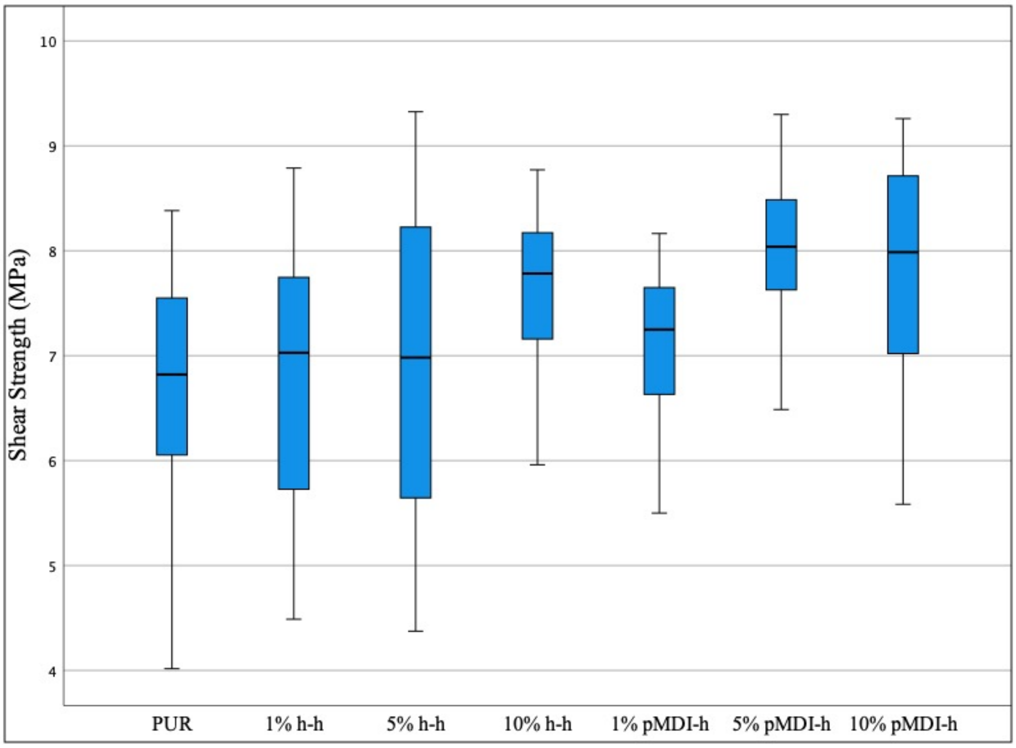

Figure 13. Shear Strength of unmodified and modified PUR at 80 °C

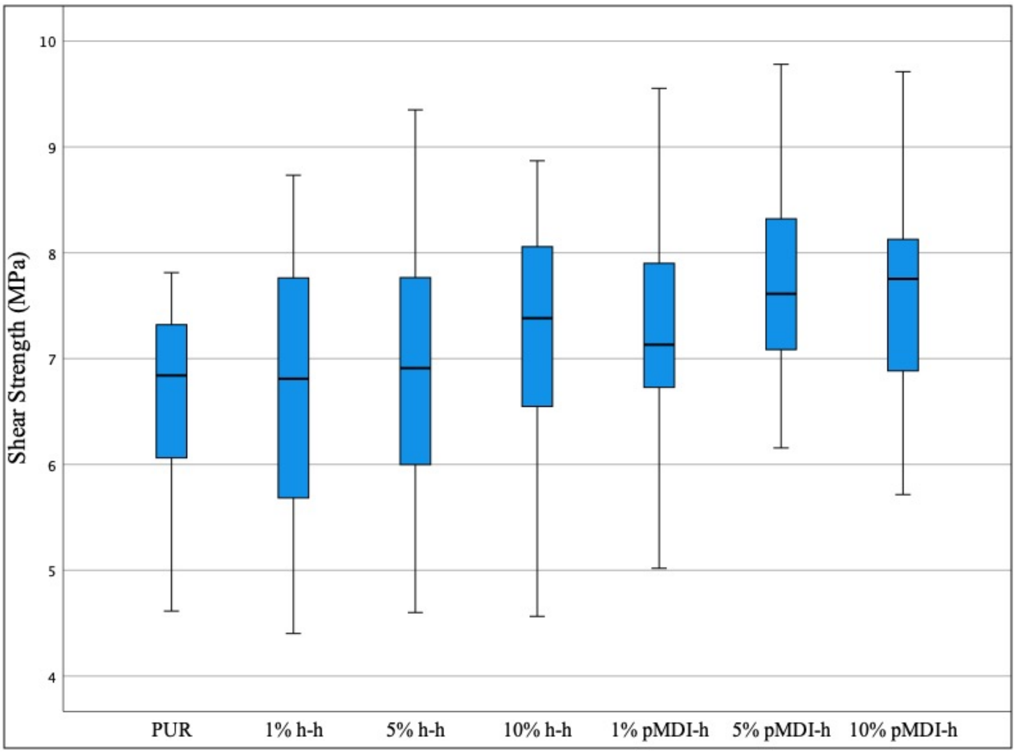

Figure 14. Shear Strength of unmodified and modified PUR at 100 °C

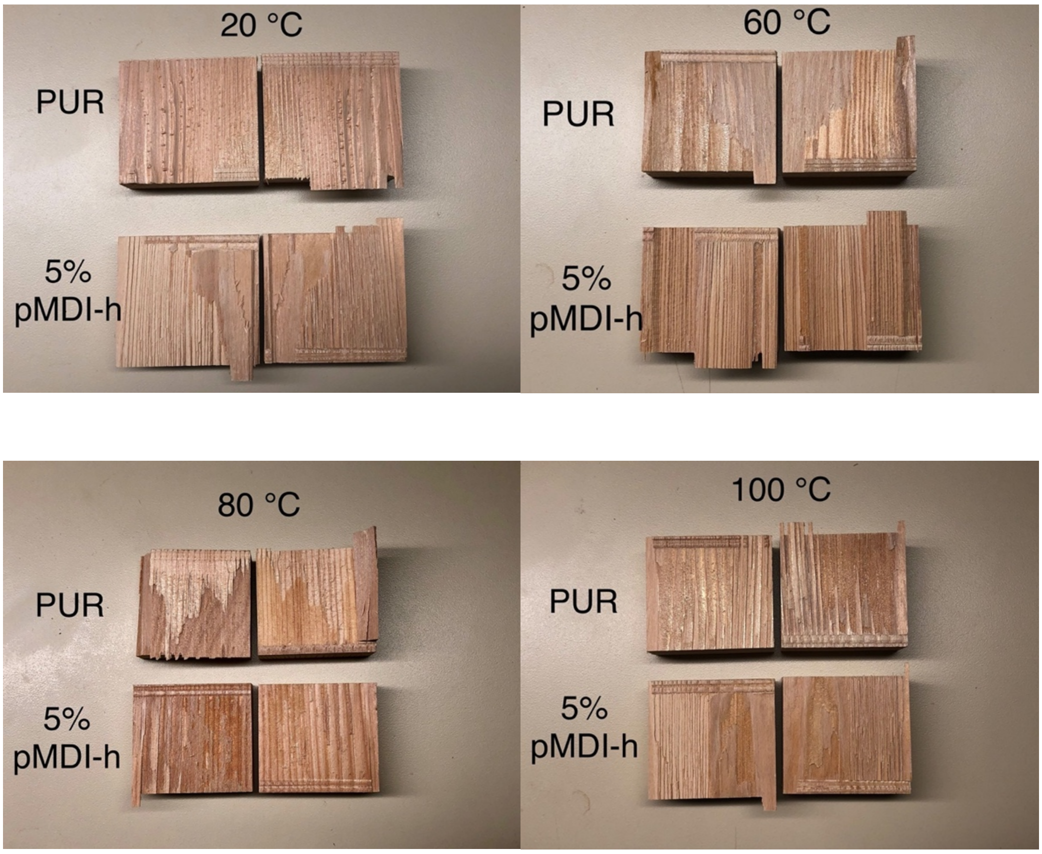

Figure 15. Pictures showing failure mode of unmodified PUR and 5% pMDI-H modified PUR adhesive at different temperatures.

3.4.2 Sprue-pine-fir

As 5% and 10% pMDI-H modified PUR adhesive showed significant improvement in the shear strength of the PUR adhesive at elevated temperature, their effects in bonding sprue-pine-fir (SPF) were also investigated at 20 and 80 °C (**Figure 16&17, Table 8&9**). As SPF species are weaker as compared to DF, the overall shear strength values are smaller. However, similar behavior can be observed for the pMDI-H modified PUR adhesive. ANOVA test showed no significant difference in the shear strength can be observed at 20 °C with the addition of 5% and 10% pMDI-H. At 80 °C, the *p*-values of 5% pMDI-H modified PUR vs. unmodified PUR and 10% pMDI-H modified PUR vs. unmodified PUR are 0.005 and <0.001, respectively, indicating both 5% and 10% pMDI-H can significantly improve the shear strength of the PUR adhesives. The average shear strength of 5% and 10% pMDI-H modified PUR adhesive at 80 °C is 27%, and 37% higher than the unmodified ones, respectively.

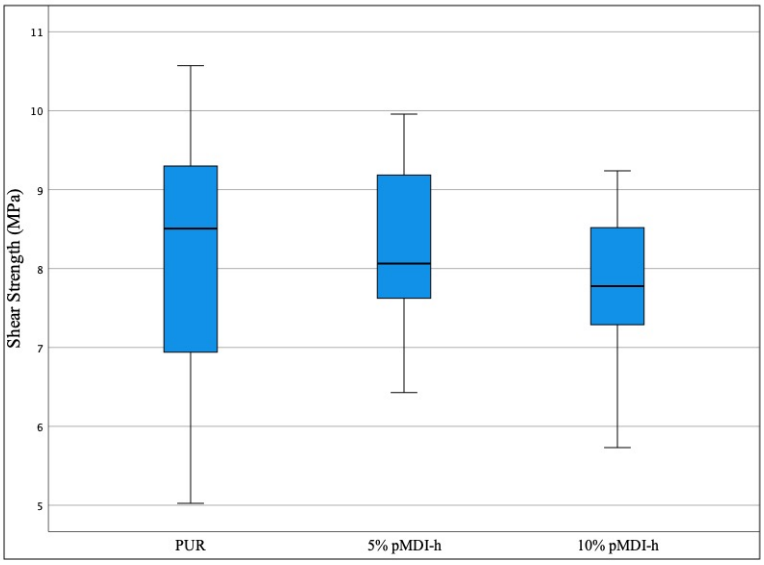

Figure 16. Shear Strength of unmodified and modified PUR at 20 °C (SPF samples)

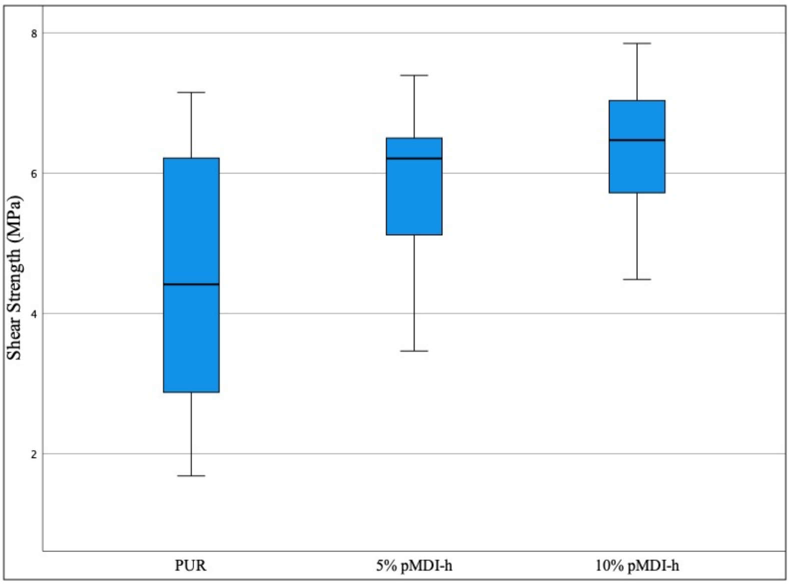

Figure 17. Shear Strength of unmodified and modified PUR at 80 °C (SPF samples)

Table 8. Statistics of the adhesive Bonding Tests-SPF at 20ºC and 80 ºC with unmodified PUR and pMDI-halloysite (pMDI-h) modified PUR.

Category	SPF-PUR (20°C)			SPF-PUR+PMDI-5% (20°C)			SPF-PUR+PMDI-10% (20°C)			SPF-PUR (80°C)				SPF-PUR+PMDI-5% (80°C)				SPF-PUR+PMDI-10% (80°C)			
	Peak Load (N)	Shear Strength (MPa)	Wood Failure (%)	Peak Load (N)	Shear Strength (MPa)	Wood Failure (%)	Peak Load (N)	Shear Strength (MPa)	Wood Failure (%)	Bond Surface Temp (°C)	Peak Load (N)	Shear Strength (MPa)	Wood Failure (%)	Bond Surface Temp (°C)	Peak Load (N)	Shear Strength (MPa)	Wood Failure (%)	Bond Surface Temp (°C)	Peak Load (N)	Shear Strength (MPa)	Wood Failure (%)
Aver.	16651	8.15	96.91	16467	8.33	96.25	16194	7.83	96.05	79.37	9450	4.55	21.1	80.91	11945	5.81	52.51	81.62	12916	6.24	55.91
Stdev	2846	1.44	4.88	1872	0.93	6.61	1684	0.82	7.03	4.04	3692	1.79	22.74	3.50	2144	1.03	25.59	2.52	2105	1.02	26.73
Max	20998	10.57	100	20388	9.96	100	19003	9.24	100	85.70	14883	7.15	86.67	86.70	15238	7.40	100	84.80	16307	7.85	100
Min	10368	5.03	84.62	12979	6.43	77.62	11982	5.73	76.19	72.50	3485	1.68	0	74.00	7097	3.46	20.28	75.40	6718	3.21	18.45
Count	30	30	30	30	30	30	30	30	30	30	30	30	30	30	30	30	30	30	30	30	30

Table 9. Comparison among groups with ANOVA for SPF samples.

Control group	Samples	20 °C			80 °C		
		Mean difference	Stdev	p-Value	Mean difference	Stdev	p-Value
PUR	5% pMDI-h	-0.17934	0.31343	0.92	-1.25944*	0.37666	0.005**
	10% pMDI-h	0.32376	0.30303	0.643	-1.69317*	0.37583	<0.001***

4. CONCLUSIONS

This research proves that the level of dispersion of halloysite in PUR adhesives can be improved by grafting pMDI onto the halloysite, and can also affect the thermal and mechanical properties of PUR adhesive. pMDI-modified halloysite showed better dispersibility than hydroxylated halloysite resulting in increased glass transition temperatures and moduli values. Similar behavior can be observed for the shear strength of the PUR glued shear blocks. 5% pMDI-H and 10% pMDI-H modified PUR adhesives significant improvement in the shear strength at elevated temperature of 60-100 ºC. These results are promising to develop thermally stable PUR adhesives systems for tall buildings.

5. REFERENCE

1. Jiang, L.; Ren, Z. Y.; Zhao, W.; Liu, W. T.; Liu, H.; Zhu, C. S., Synthesis and structure/properties characterizations of fou polyurethane model hard segments. *Royal Society Open Science* **2018,** *5* (7).
2. Solt, P.; Konnerth, J.; Gindl-Altmutter, W.; Kantner, W.; Moser, J.; Mitter, R.; van Herwijnen, H. W. G., Technological performance of formaldehyde-free adhesive alternatives for particleboard industry. *International Journal of Adhesion and Adhesives* **2019,** *94*, 99-131.
3. Van de Kuilen, J. W. G.; Ceccotti, A.; Xia, Z. Y.; He, M. J., Very Tall Wooden Buildings with Cross Laminated Timber. *Proceedings of the Twelfth East Asia-Pacific Conference on Structural Engineering and Construction (Easec12)* **2011,** *14*, 1621-1628.
4. Muszynski, L.; Gupta, R.; Hong, S. H.; Osborn, N.; Pickett, B., Fire resistance of unprotected cross-laminated timber (CLT) floor assemblies produced in the USA. *Fire Safety Journal* **2019,** *107*, 126-136.
5. Zelinka, S. L.; Sullivan, K.; Pei, S. L.; Ottum, N.; Bechle, N. J.; Douglas, R. R.; Hasburgh, L. E., Small scale tests on the performance of adhesives used in cross laminated timber (CLT) at elevated temperatures. *International Journal of Adhesion and Adhesives* **2019,** *95*.
6. Goda, E. S.; Yoon, K. R.; El-sayed, S. H.; Hong, S. E., Halloysite nanotubes as smart flame retardant and economic reinforcing materials: A review. *Thermochimica Acta* **2018,** *669*, 173-184.

7. Smith, R. J.; Holder, K. M.; Ruiz, S.; Hahn, W.; Song, Y. X.; Lvov, Y. M.; Grunlan, J. C., Environmentally Benign Halloysite Nanotube Multilayer Assembly Significantly Reduces Polyurethane Flammability. *Advanced Functional Materials* **2018,** *28* (27).

8. Carosio, F.; Cuttica, F.; Medina, L.; Berglund, L. A., Clay nanopaper as multifunctional brick and mortar fire protection coating-Wood case study. *Materials & Design* **2016,** *93*, 357-363.

9. Guo, B. T.; Liu, Y. Z.; Zhang, Q.; Wang, F. Q.; Wang, Q. W.; Liu, Y. X.; Li, J.; Yu, H. P., Efficient Flame-Retardant and Smoke-Suppression Properties of Mg-Al-Layered Double-Hydroxide Nanostructures on Wood Substrate. *Acs Applied Materials & Interfaces* **2017,** *9* (27), 23039-23047.

10. Feitosa, S. A.; Munchow, E. A.; Al-Zain, A. O.; Kamocki, K.; Platt, J. A.; Bottino, M. C., Synthesis and characterization of novel halloysite-incorporated adhesive resins. *Journal of Dentistry* **2015,** *43* (11), 1316-1322.

11. Leitune, V. C. B.; Collares, F. M.; Trommer, R. M.; Andrioli, D. G.; Bergmann, C. P.; Samuel, S. M. W., The addition of nanostructured hydroxyapatite to an experimental adhesive resin. *Journal of Dentistry* **2013,** *41* (4), 321-327.

12. Deng, S. Q.; Zhang, J. N.; Ye, L.; Wu, J. S., Toughening epoxies with halloysite nanotubes. *Polymer* **2008,** *49* (23), 5119-5127.

13. Qi, X. G.; Zhang, Y. S.; Chang, C.; Luo, X. L.; Li, Y. B., Thermal, Mechanical, and Morphological Properties of Rigid Crude Glycerol-Based Polyurethane Foams Reinforced With Nanoclay and Microcrystalline Cellulose. *European Journal of Lipid Science and Technology* **2018,** *120* (5).

14. Zeng, S. S.; Reyes, C.; Liu, J. J.; Rodgers, P. A.; Wentworth, S. H.; Sun, L. Y., Facile hydroxylation of halloysite nanotubes for epoxy nanocomposite applications. *Polymer* **2014,** *55* (25), 6519-6528.